

Light extraction beyond total internal reflection using one-dimensional plasmonic crystals

R. McCarron,^{a)} D. O'Connor, J.-S. Bouillard, W. Dickson, and A. V. Zayats

Nano-optics and Near-field Spectroscopy Group, Department of Physics, King's College London, Strand, London WC2R 2LS, United Kingdom

(Received 18 May 2011; accepted 3 August 2011; published online 24 August 2011)

We demonstrate the application of plasmonic crystals for extracting light trapped in the substrate due to total internal reflection (TIR). The broadband transmission properties of one-dimensional plasmonic crystals have been investigated, both experimentally and numerically, beyond the TIR critical angle in order to reveal the role of plasmonic modes in this process. Through optimisation of the traditional square slit unit cell geometry of the crystals, transmission coefficients of up to 47% were obtained in the TIR regime. An U-shaped cell geometry with a few nm thick continuous film was found to significantly modify the plasmonic modes of the crystal in addition to exhibiting highly tuneable, structurally dispersive transmission peaks, further increasing transmission in the TIR regime up to 56%. Such structures exhibit better than glass transparency at the design wavelength when integrated over all incident angles. © 2011 American Institute of Physics. [doi:10.1063/1.3628330]

The coupling of light to surface plasmon polaritons (SPPs) has been shown to improve the far field optical transmission through nanostructured metallic films.¹⁻³ So-called surface plasmon polaritonic crystals (SPPCs) provide an efficient tuneable coupling mechanism through which this SPP-mediated transmission may be enhanced,²⁻⁴ yet the potential industrial application of SPPCs has been limited largely to colour filtering^{5,6} and polarisation control.^{7,8} A significant opportunity exists to exploit the enhanced transmission properties of plasmonic crystals in photonic devices such as organic and inorganic light emitting diodes (OLEDs/LEDs) to increase the extraction of light trapped due to the total internal reflection (TIR) in the active material. Up to 95% of the light generated in the emissive layer cannot be extracted as a result of their inherently high refractive indices, e.g., $n \sim 3.6$ in the case of gallium phosphide in the visible spectral range, leading to a TIR critical angle of just 14.8° .⁹ Solutions to this problem have included micro patterning of the semiconductor surface¹⁰ and also reconfiguration of the device geometry.^{11,12} SPPCs may provide an alternative to these mechanisms for light extraction while also adding functionalities such as built in polarisation and directionality control and the possibility to utilize the entire surface for electric contact purposes.¹³

In the past, the transmission properties of plasmonic crystals were studied primarily in the range of incident angles where zero-order transmission is important. In this letter, we investigate, both experimentally and numerically, the transmission properties of one-dimensional (1D) plasmonic crystals on glass substrates and in particular the role of the crystal's unit cell geometry. We show that plasmonic crystals can extract a significant portion of the light otherwise trapped by TIR. This is important for applications in LED and OLED devices as well as high-resolution optical imaging.

The plasmonic crystals used in this study were fabricated by focused-ion-beam milling of square profile slits in a 100 nm thick Au film that was magnetron sputtered onto glass substrates (Fig. 1). The periodicity of the unit cell and total size of each crystal was held constant at 600 nm and $15 \times 15 \mu\text{m}^2$, respectively, while the profile of the slits in different crystals was varied with different widths and depths. Optical characterisation was performed by illuminating the sample with collimated p-polarised white-light through a hemispherical glass prism and collecting far-field transmission spectra at varying angles of incidence. The range of incident angles was limited to 0° – 52° . An objective lens with optical axis normal to the sample surface with a

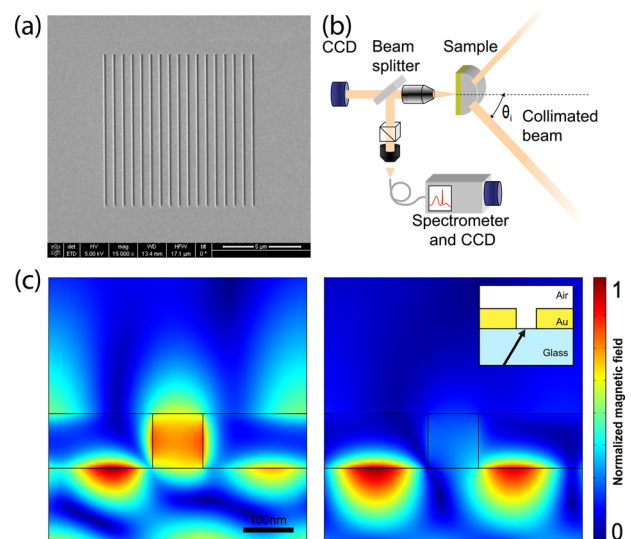


FIG. 1. (Color online) (a) SEM images of the SPP crystal (600 nm period, 140 nm width slits) in 100 nm thick Au film. (b) Experimental set-up for transmission analysis of the crystals. (c) The magnetic field intensity distributions generated by the SPP crystal with the parameters above for the (1,0) SPP Bloch modes on (left) the Au-air interface ($\lambda = 600$ nm) and (right) the Au-glass interface ($\lambda = 695$ nm) at under illumination 48° angle of incidence from substrate (inset: schematic cross section of structure with illumination).

^{a)} Author to whom correspondence should be addressed. Electronic mail: ryan.mccarron@kcl.ac.uk.

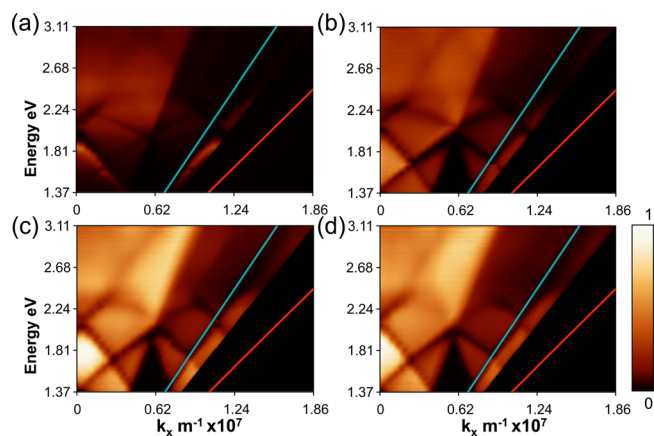


FIG. 2. (Color online) Experimentally measured transmission dispersion of plasmonic crystals (period 600 nm) for the slit width (a) 140 nm, (b) 250 nm, (c) 300 nm, and (d) 350 nm. Light line in air (blue, upper line) corresponding to outset of the TIR regime, and glass (red, lower line) are also shown. The color scale indicating transmission is the same for all plots.

numerical aperture of 0.5 was used to collect the light, which was separated via a beam splitter and sent to both a camera for real-time observation of structure location and to the spectrometer via an optical fibre. The collection angle of the objective was $\pm 30^\circ$.

Numerical modelling was performed using finite element method. Only a single unit cell was simulated by exploiting Floquet theory (the 1D form of Bloch's theorem) to provide boundary conditions allowing the efficient investigation of the optical response of infinite crystals with parameterised unit cell geometry, using complex refractive index data from Ref. 14. The collected spectra from both experiment and simulation were processed to plot the transmission dispersion.

Figures 2 and 3 show a selection of the experimentally measured and simulated dispersion plots from SPPCs with different slit widths (note that the model dispersions were simulated for wider range of the incident angles which was limited in the experiment). The light lines in air and glass show the maximum wave vectors achievable in the superstrate and substrate and hence the region between these corresponds to the TIR regime. The simulated and measured dispersion are in very good agreement with each other taking into account the experimental conditions. Please note that the measured dispersions exhibit some reduction in transmittance beyond 30° angle of incidence due to zero-order transmission falling outside the collection objective acceptance angle, visible as a transition in brightness in all dispersion plots in Fig. 2. The limited acceptance angle further provides the dark triangular region at the transition point, due to overlapping regions of non-zero-order transmission in subsequent Brillouin zones.

The transmission dispersions exhibit the typical Bloch mode characteristics of a plasmonic crystal which follow the approximate relation for Bragg-scattered SPPs in this periodic system.¹⁵ In all cases, there is a significant transmittance of light beyond the critical angle and thus, the presence of these plasmonic crystals indeed enables the outcoupling of light otherwise trapped in the substrate. For the structures analysed, increasing the trench width from 140 nm to 350 nm results in a general increase in transmittance and band-gap

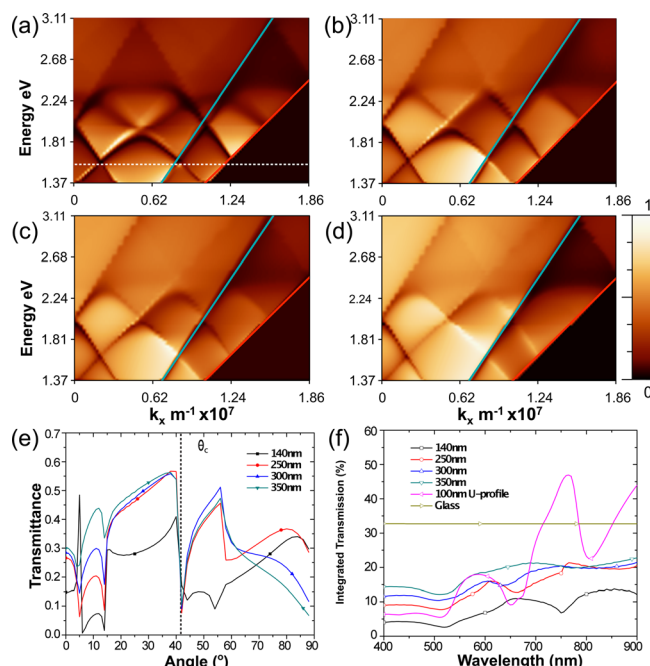


FIG. 3. (Color online) (a)-(d) Simulated transmission dispersion of plasmonic crystals with the parameters as in Fig. 2. The color scale is the same for all plots. (e) Transmittance at the 825 nm wavelength for all gratings and a bare glass substrate (cross section of (a)-(d) represented by the dashed line in (a)). (f) Angular-integrated transmission for all gratings analysed as a comparison to a bare glass substrate; U-profile has 5 nm underlayer.

definition. This can be attributed to changes in the SPP scattering properties of the slits.

The simulations show that this additional transmission (up to 60%) beyond the critical angle is maintained up to the angle of incidence approaching 90° . It can be seen from Fig. 3(e) that beyond the critical angle and the narrow range of the angles with small transmission, the transmission is almost constant. Increasing the slit width leads to further improvement in outcoupling at smaller angles.

To compare SPPC mediated outcoupling to that of an uncoated substrate, the angular transmission data for each wavelength were integrated over the whole range of incident angles, giving a wavelength-dependant total transmission (Fig. 3(f)). The integrated transmission increases with the slit width reaching about 20%, compared to the 30% of the integrated transmission of the bare glass substrate. The latter is high due to the strong transmission at the incidence angles close to the normal. The use of the crystal however provides control over the directionality of the outcoupled light.

The ability to engineer the dispersion of the SPP modes existing on such structures was demonstrated on plasmonic crystals having slits of a depth approaching the film thickness but not fully perforating the metal. The effect of varying the profile of such imperforated U-shaped gratings provides a very sensitive method of tailoring the optical response of the structure.

Figure 4(a) shows the simulated far-field transmission dispersion of a U-shaped groove grating. The formation of a strongly resonant, flat plasmonic band is evident at the boundary of the first Brillouin zone at an energy corresponding to a band gap of the substrate SPP Bloch modes. This is associated with a strong coupling of the localised plasmonic resonance of the U-shaped cavity and the Bloch modes,

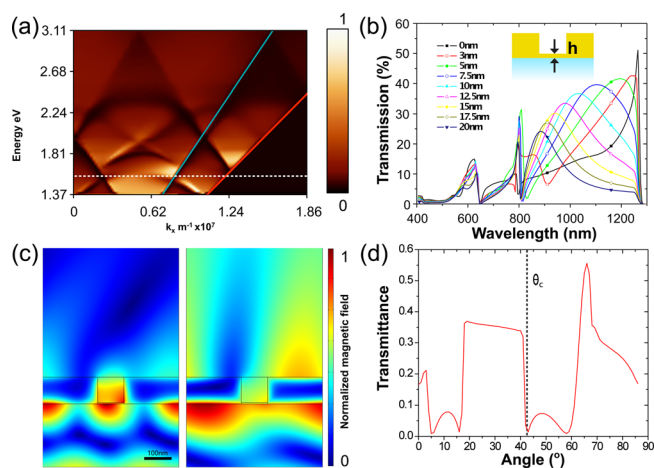


FIG. 4. (Color online) (a) Transmission dispersion of a 600 nm period SPPC in 100 nm Au film with a 5 nm underlayer on a glass substrate. (b) Variation of transmission spectra with the underlayer thickness for 48° angle of incidence. The inset shows the schematic of the SPPC consisting of the U-shaped features. (c) The magnetic field intensity distribution for the SPPC in (a) at $\lambda = 720$ nm (left) and $\lambda = 1070$ nm (right) at 48° angle of incidence. (d) SPPC transmittance at the 865 nm wavelength represented by the dashed line in (a).

resulting in a typical anticrossing of the resonances clearly observed in the dispersion (Fig. 4(a)). This leads to the flat bands in the dispersion and thus omnidirectional response of the structure at around this resonance (Fig. 4(d)). The simulated field plots show a strong field confinement and enhancement on this underlayer in confirmation of this and may have application in sub-attolitre sensing and nonlinear devices (Fig. 4).

Upon examining the optical response of this structure at an angle beyond total internal reflection, a strong transmission peak is observed that is tuneable in a broad spectral range by varying the depth of the groove (Fig. 4(b)). This near-infrared transmission peak exhibits a blue-shift with increasing thickness of the layer, behaving much like the longitudinal resonance of an effective particle with decreasing aspect ratio.¹⁶ Over the 400–1700 nm wavelength range, the U-shaped grating has a maximum of 56% transmission, compared to 53% for the perforated slits. The integrated transmission in this case reaches about 45% at certain wavelengths exceeding the transmission of the smooth substrate (Fig. 3(f)).

In summary, the extraction of light from a substrate using 1D plasmonic crystals was investigated. Far field transmission

dispersion plots showed typical plasmonic features and exhibited significantly increased transmission beyond TIR reaching up to 60%. Most interestingly, U-shaped groove gratings displayed strong localised plasmonic resonances and additional transmission peaks in TIR regime that were tuneable in a broad spectral range. Such a substructure is more transparent than glass with total transmission up to 45% at the designed wavelength. The enhancement exhibited by these structures will become even more significant in 3D, when accounting for emission into a solid angle (only about 13% and 3% transmission for bare glass and GaP, respectively, is achievable in this case). Plasmonic crystals show significant potential for increasing the output efficiency of LEDs both in the IR and visible regimes with additional benefits of achieving directionality engineering and contact layers transparency.

This work was supported in part by EPSRC (UK) and EC FP6 project PLEAS.

- ¹T. W. Ebbesen, H. J. Lezec, H. F. Ghaemi, T. Thio, and P. A. Wolff, *Nature (London)* **391**, 667 (1998).
- ²L. Martin-Moreno, F. J. Garcia-Vidal, H. J. Lezec, K. M. Pellerin, T. Thio, J. B. Pendry, and T. W. Ebbesen, *Phys. Rev. Lett.* **86**, 1114 (2001).
- ³L. Salomon, F. Grillot, A. V. Zayats, and F. de Fornel, *Phys. Rev. Lett.* **86**, 1110 (2001).
- ⁴A. V. Zayats, I. I. Smolyaninov, and A. A. Maradudin, *Phys. Rep.* **408**, 131 (2005).
- ⁵E. Laux, C. Genet, T. Skauli, and T. W. Ebbesen, *Nat. Photonics* **2**, 161 (2008).
- ⁶Z. P. Yang and S. Y. Lin, *Opt. Lett.* **34**, 3893 (2009).
- ⁷N. Yu, Q. J. Wang, C. Pflugl, L. Diehl, F. Capasso, T. Edamura, S. Furuta, M. Yamanishi, and H. Kan, *Appl. Phys. Lett.* **94**, 151101 (2009).
- ⁸M. Guillaumee, L. A. Dunbar, C. Santschi, E. Grenet, R. Eckert, O. J. F. Martin, and R. P. Stanley, *Appl. Phys. Lett.* **94**, 193503 (2009).
- ⁹S. Adachi, *J. Appl. Phys.* **66**, 6030 (1989).
- ¹⁰H. W. Huang, F. I. Lai, J. K. Huang, C. H. Lin, K. Y. Lee, C. F. Lin, C. C. Yu, H. C. Kuo, and H. C. Kuo, *Semicond. Sci. Technol.* **25**, 065007 (2010).
- ¹¹K. H. Kim, J. H. Shin, N. M. Park, C. Huh, T. Y. Kim, K. S. Cho, J. C. Hong, G. Y. Sung, and G. Y. Sung, *Appl. Phys. Lett.* **89**, 191120 (2006).
- ¹²W. K. Wang, D. S. Wu, S. H. Lin, S. Y. Huang, P. Han, and R. H. Horng, *Jpn. J. Appl. Phys.* **45**, 3430 (2006).
- ¹³A. Drezet, F. Przybilla, E. Laux, O. Mahboub, C. Genet, T. W. Ebbesen, I. S. Spevak, A. V. Zayats, A. Y. Nikitin, and L. Martin-Moreno, *Appl. Phys. Lett.* **95**, 021101 (2009).
- ¹⁴*Handbook of Optical Constants of solids*, edited by E. D. Palik (Academic, New York, 1984).
- ¹⁵W. Dickson, G. A. Wurtz, P. R. Evans, R. J. Pollard, I. S. Spevak, and A. V. Zayats, *Nano Lett.* **8**, 281 (2008).
- ¹⁶R. M. Boardman, *Electromagnetic Surface Modes* (Wiley, New York, 1982).